www.elsevier.com/locate/jep

Effects and mechanisms of Shaofu-Zhuyu decoction and its major bioactive component for Cold - Stagnation and Blood – Stasis primary dysmenorrhea rats

Xiaochen Huang, Shulan Su, Jin-ao Duan, Xiuxiu Sha, Kavin Yue Zhu, Jianming Guo, Li Yu, Pei Liu, Erxin Shang, Dawei Qian

PII: S0378-8741(16)30186-6
DOI: http://dx.doi.org/10.1016/j.jep.2016.03.067
Reference: JEP10074

To appear in: *Journal of Ethnopharmacology*

Received date: 20 August 2015
Revised date: 26 January 2016
Accepted date: 31 March 2016

Cite this article as: Xiaochen Huang, Shulan Su, Jin-ao Duan, Xiuxiu Sha, Kavi Yue Zhu, Jianming Guo, Li Yu, Pei Liu, Erxin Shang and Dawei Qian, Effects and mechanisms of Shaofu-Zhuyu decoction and its major bioactive componer for Cold - Stagnation and Blood – Stasis primary dysmenorrhea rats, *Journal o Ethnopharmacology,* http://dx.doi.org/10.1016/j.jep.2016.03.067

Effects and mechanisms of Shaofu-Zhuyu decoction and its major bioactive component for Cold - Stagnation and Blood – Stasis primary dysmenorrhea rats

Xiaochen Huang[1,2], Shulan Su[1]*, Jin-ao Duan[1]*, Xiuxiu Sha[1], Kavin Yue Zhu[1], Jianming Guo[1], Li Yu[1], Pei Liu[1], Erxin Shang[1], Dawei Qian[1]

(1. *Jiangsu Key Laboratory for High Technology Research of TCM Formulae, Jiangsu Collaborative Innovation Center of Chinese Medicinal Resources Industrialization, Nanjing University of Chinese Medicine, Nanjing 210023, China;* 2. *Nanjing University of Chinese Medicine Hanlin College, Taizhou, 225300, China*)

*Corresponding author. Dr. Shulan Su and Prof. Jin-ao Duan

Jiangsu Key Laboratory for High Technology Research of TCM Formulae, Nanjing University of Chinese Medicine, Nanjing 210046, PR China

Tel. / fax: +86 25 85811916

E-mail: sushulan1974@163.com

Tel. / fax: +86 25 85811116

E-mail: duanja@163.com

Abstract

Ethnopharmacological relevance:

Traditional Chinese medicine (TCM) is used under the guidance of the theory of traditional Chinese medical sciences in clinical application. The Chinese herbal formula, Shaofu Zhuyu decoction (SFZYD), is considered as an effective prescription for treating Cold - Stagnation and Blood – Stasis (CSBS) primary dysmenorrhea. The previous studies showed the SFZYD exhibited great anti-inflammation and analgesic effect. In this present study the metabolomics of CSBS primary dysmenorrhea diseased rats and the cytokine transcription in PHA stimulated-PBMC were investigated to explore the effects and mechanisms.

Aim of the study:

Explore a valuable insight into the effects and mechanisms of SFZYD for Cold - Stagnation and Blood – Stasis primary dysmenorrhea rats.

Materials and methods:

We established CSBS primary dysmenorrhea diseased rats according the clinical symptoms. A targeted tandem mass spectrometry (MS/MS)-based metabolomic platform was used to evaluate the metabolic profiling changes and the intervention by SFZYD. The PBMC cell was adopted to explore the mechanisms by analyzing the signaling pathway evaluated by expression of inflammatory cytokines, c-jun and c-fos and corresponding phosphorylation levels.

Results:

Estradiol, oxytocin, progesterone, endothelin, β-endorphin and $PGF_{2\alpha}$ were restored back to the normal level after the treatment of SFZYD. Total twenty-five metabolites (ten in plasma and fifteen in urine), up-regulated or down-regulated, were identified. These identified biomarkers underpinning the metabolic pathway including pentose and glucuronate interconversions, steroid hormone biosynthesis, and glycerophospholipid metabolism are disturbed in model rats. Among these metabolites, twenty one potential biomarkers were regulated after SFZYD treated. The compound of paeoniflorin, a major bioactive compound in SFZYD, was proved to regulate the MAPK signaling pathway by inhibiting the expression of IL-1β, IL-2, IL-10, IL-12, TNFα, INFγ, C-jun and C-fos in PHA stimulated-PBMC.

Conclusion:

These findings indicated that SFZYD improved the metabolic profiling and biochemical indicators on CSBS primary dysmenorrhea rats. And the mechanisms were closely related with the regulation of the MAPK pathway by reduction in phosphorylated forms of the three MAPK (ERK1/2, p38 and JNK) and down regulation of *c-jun* and *c-fos* by paeoniflorin. The data could be provided the guidance for further research and new drug discovery.

Keywords: primary dysmenorrhea (PD), Shaofu Zhuyu decoction (SFZYD), UPLC−QTOF-MS/MS, metabolomics, potential biomarkers, MAPK signaling pathway

Abbreviations:

TCM (Traditional Chinese medicine)

SFZYD (Shaofu Zhuyu decoction)

CSBS (Cold - Stagnation and Blood – Stasis)

PBMC (peripheral blood mononuclear cells)

PD (primary dysmenorrhea)

MAPK (mitogen-activated protein kinases)

NSAIDs (Nonsteroidal anti-inflammatory drugs)

PCR (Polymerase Chain Reaction)

UPLC (Ultra high Performance Liquid Chromatography)

1. Introduction

Traditional Chinese Medicine (TCM), which has been proved to be effective and safe in clinical applications for thousands of years, is considered as a feasible alternative treatment for PD (Hsu et al., 2006). Shao-Fu-Zhu-Yu Decoction (SFZYD) is considered as an effective prescription for treating PD. This prescription originally came from "Correction of Errors in Medical Classics" compiled by Qing-ren Wang in Qing dynasty (A.D. 1830). The formula includes the following ten herbs: Angelicae sinensis Radix, Chuanxiong Rhizoma, Corydalis Rhizoma, Foeniculi Fructus, Zingiberis Rhizoma, Myrrha, Trogopteri Feces, Typhae Pollen, Paeoniae Radix Rubra, and Cinnamomi Cortex, respectively. It has been used in clinic to treat blood stasis syndrome of gynecology diseases such as dysmenorrhea for about 200 years and effective (Fan et al., 2011; Cheng et al., 2011). Our previous researches also indicated that SFZYD showed an inhibition of uterine smooth muscle constriction and manifested an anti-inflammatory activity (Su et al., 2010). Recent study showed that SFZYD could significantly improve the outer membrane of uterus microcirculation and blood coagulation function of rat with blood stasis (Su et al., 2010). Furthermore, the metabonomics study in patients affected by PD has given clinical evidence that SFZYD prevents and benefits many disorders throughout the body (Su et al., 2013). However, the therapeutic mechanisms of SFZYD still need comprehensive investigation.

PD is one of the most common gynaecological disorders in young women (Doubova et al., 2007; Wolf et al., 1999). With symptoms becoming severe, it will

lead to a lot of problems (French et al., 2005; Davis et al., 2005). Traditional Chinese physician treat PD based on an overall analysis of the illness and the patient's condition, and primary dysmenorrhea of CSBS type is considered the most common.

The pathogenesis of PD is not precisely understood. However, theories proposed by available data mostly congregate on the excessive secretion of uterine prostaglandins (PGs) for the underlying cause of PD (Chan et al., 1980). Therefore, some medications specific to decrease the production of PGs are applied to relieve the symptoms. Nonsteroidal anti-inflammatory drugs (NSAIDs) are the most common pharmacologic treatments for PD. Moreover, PD has also been suggested to be a sex-hormone and ovarian steroids related disorder (Ostad et al., 2001). So some other methods such as oral contraceptive pills and Mirena were applied for treating PD. The efficacy of these drugs is obvious and rapid, but a certain number of women affected by PD do not respond to these medicines and be allergic to these medications. Furthermore, they are intolerable and have plenty of side effects that affect gastrointestinal, hepatic, renal, and even cardiac systems (Zahradnik et al., 2010; Davis et al., 2005; Proctor et al., 2001).

PD is associated with inflammation, and when inflammation occurs, some cytokines, chemokines, growth factors, and other mediators are produced and the leukocytes are recruited to the area of injury or infection (Kracht et al., 2002; White et al., 2005; Moss et al., 2005). Thus, the cytokine antagonists may have significant therapeutic efficacy in several areas of cancer therapy and inflammatory diseases (Balkwill et al., 2001). Some chemical compound block TNF signaling and synthesis

such as the inhibitors of p38 MAPK is under clinical evaluation (Yan et al., 2006). Furthermore, anti-pro-inflammatory cytokine therapy has been regarded as a potential anti-inflammatory treatment (Baggio et al., 2005; Hougee et al., 2005).

Metabolomics is very useful for diagnosing and monitoring disease progression. However, there are few reports of metabolic profiling or biomarkers researches on PD, except Su and Liu (Su et al., 2013; Liu et al., 2013). Metabolomics has been used for the analysis of low molecular weight compounds to systematic investigation of metabolic responses in biological systems to genetic or environmental stimuli (Nicholson et al., 2012).

In this paper, the metabolic profiling changes were investigated based on UPLC-QTOF/MS/MS in order to discover the potential biomarkers for Cold - Stagnation and Blood – Stasis primary dysmenorrhea rats and explore the action mechanisms of SFZYD. Furthermore, we explored the effects of paeoniflorin (a major bioactive compound in SFZYD) on IL-1β, IL-2, IL-10, IL-12, TNFα, INFγ, C-jun and C-fos expression in PHA stimulated-PBMC (peripheral blood mononuclear cell) and to explore the regulation of possible signaling pathways.

2. Materials and Methods

2.1 SFZYD preparation

Two kilogram raw materials of Angelicae sinensis Radix, Chuanxiong Rhizoma, Paeoniae Radix Rubra, Cinnamomi Cortex, Foeniculi Fructus, Zingiberis Rhizoma, Myrrha, Trogopteri Feces, Typhae Pollen, and Corydalis Rhizoma were mixed at a weight ratio of 3:1:2:1:0.5:2:1:3:1:1. The herbal admixture was decocted with 20 L of

water for 2 h. The filtrates were collected and the residues were decocted in 16 L of water for 1.5 h. The filtrates from each decoction were combined and freeze-dried into a powder.

The raw materials Angelicae sinensis Radix is derived from the root of *Angelica sinensis* (Oliv.) Diels., which belongs to family of Umbelliferae, and were purchased from Minxian (Gansu). Chuanxiong Rhizoma is derived from the rhizoma of *Ligusticum chuanxiong* Hort., which belongs to family of Umbelliferae, and were purchased from Pengzhou (Sichuan). Paeoniae Radix Rubra is derived from the root of *Paeonia lactiflora* Pall., which belongs to family of Ranunculaceae, and were purchased from Chifeng (Neimeng). Cinnamomi Cortex is derived from the bark of *Cinnamomum cassia* Presl., which belongs to family of Lauraceae, and were purchased from Yulin (Guangxi), Foeniculi Fructus is derived from the fruits of *Foeniculum vulgare* Mill., which belongs to family of Umbelliferae, and were purchased from Wuwei (Gansu). Zingiberis Rhizoma is derived from the rhizoma of *Zingiber offcinale* Rosc., which belongs to family of Zingiberaceae, and were purchased from Yulin (Guangxi). Myrrha is derived from the resin of *Commiphora myrrha* Engl., which belongs to family of Buseraceae, and were purchased from Guangdong, Trogopteri Feces is derived from the faeces of the complex-toothed flying squirrel *Trogopterus xanthipes* Milne-Edwards belongs to family of Petauristidae, and were purchased from Changzhi (Shanxi). Typhae Pollen is derived from the pollen of *Typha angustifolia* L., which belongs to family of Typhaceae, and were purchased from Jiangsu (Yixing), and Corydalis Rhizoma is derived from the tuber of *Corydalis*

yanhusuo W.T.Wang., which belongs to family of Papaveraceae, and were purchased from Songyang (Zhejiang), respectively. The corresponding author authenticated all of the raw materials, and the herbal drugs were verified according to the Chinese pharmacopeia (Chinese pharmacopeia, 2010). These voucher specimens (No. NJUTCM - 20120518-20120527) were deposited in the Jiangsu Key Laboratory for TCM Formulae Research of Nanjing University of Chinese Medicine.

2.2 Animal handing and grouping

Sprague Dawley rats (weighting 200 ± 20 g) were supplied by the Good Laboratory Practice Center of Nanjing University of Chinese Medicine (Nanjing, China). The room temperature was regulated at 25 ± 1 °C with 50 ± 5% humidity. A 12-h light/dark cycle was set, with free access to standard diet and water. All rats were randomly divided into 3 groups of 8 rats each as follows: control group, primary dysmenorrhea group and SFZYD treatment group. The primary dysmenorrhea group and SFZYD treatment group were swimming in the 0-4 °C ice-water and had subcutaneous injection of estradiol benzoate 1mg per kilogram for seven consecutive days. Therefore, on the eighth day, rats had intraperitoneal injection of epinephrine twice interval four hours, and the measurement is 0.16mg each, and then, intraperitoneal injection of oxytocin 1mg per kilogram. The SFZYD treatment group was orally administrated with SFZYD and the control group was orally administrated with an equivalent volume of distilled water.

2.3 Animal plasma and urine samples

All plasma sample purification was limited to protein precipitation with methanol.

100 μL plasma samples were extracted with 400 μL methanol. After vortex for 1min and centrifugation at 13 000 × g for 10 min, most protein was removed and the mixture solution was filtered through a PTFE membrane of 0.22 mm. Urine samples were thawed at room temperature and centrifuged at 5000 × g for 10 min. The supernatant liquid 1 mL was added to 3 mL methanol and vortex mixed for 30 s, then centrifuged at 13 000 × g for 10 min to obtain the supernatant. The supernatant was filtered through 0.22 mm PTFE membrane. All samples were transferred to an auto sampler vial kept at 4 1C and an aliquot of 5 mL was injected for LC/MS analysis.

2.4 Biochemical indicators measurements

The therapeutic efficacy was evaluated for the levels of estradiol, oxytocin, progesterone, endothelin, prostaglandin E_2 (PGE_2), β-endorphin and prostaglandin F_2 (PGF_2) in plasma. Biochemical analysis data were presented as the mean ± SD. Statistical significance was assessed by ANOVA test and Shapiro-Wilk statistics was adopted to test normal distribution by SPSS 16.0 version (Inc., Chicago, IL). In all experiments, confidence level was set at 95% to determine the significance of difference ($P < 0.05$).

2.5 Chromatography and mass spectrometry conditions

Samples were run in a random, non-grouped order. The UPLC analysis was performed on a Waters ACQUITY UPLC system (Waters Corporation, Milford, USA). Acquity UPLC BEHC18 column (2.1 mm × 100 mm, 1.7 mm) was applied for all analyses. The mobile phase was composed of acetonitrile (A) and 0.1% formic acid, v/v (B). For plasma analysis, the mobile phase with a linear gradient elution: 0–4 min,

A: 95-64%; 4–5 min, A: 64–35%; 5-11 min, A: 35–10%; 11–12 min, A: 10–10%; 12–13 min, A: 10–95%. For urine analysis, the mobile phase with a linear gradient elution: 0–10 min, A: 95-70%; 10–11 min, A: 70-5%; 11–12 min, A: 5-5%; 12–13 min, A: 5–95%. The flow rate of the mobile phase was 0.4 mL min^{-1}, and the column temperature was maintained at 35 °C.

MS was performed on a Synaptt Q-TOF (Waters, Manchester, UK). The instrument was operated by using an electrospray ionization (ESI) source in positive mode. The ionization source conditions were as follows: capillary voltage of 3.0 kV, source temperature of 120 °C and desolvation temperature of 35 °C. The MS data were collected from m/z 100 to 1000 Da in positive ion in centroid mode. Data acquisition and processing were performed by using Masslynxt v 4.1 (Waters Corporation).

2.6 Pattern recognition analysis and data processing

The mass data acquired were imported to Markerlynx within Masslynx software (version 4.1) for peak detection and alignment. The retention time and *m/z* data for each peak were determined by the software. The parameters of Markerlynx method were set as follows: mass tolerance 0.1 Da; noise elimination level 5; full scan mode was employed in the mass range of 100-1000 amu; the initial and final retention times were set as 0 and 12 min for data collection. All data were normalized to the summed total ion intensity per chromatogram, and the resultant data matrices were introduced to *EZinfo* 2.0 software for principal component analysis (PCA), partial least-squaresdiscriminant analysis (PLS-DA) and orthogonal projection to latent structures (OPLS) analysis. Prior to PCA, all variables obtained from LC- MS data

sets were mean-centered and scaled to Pareto variance. PCA is an unsupervised multivariate statistical approach. It is used for variable reduction and separation into classes. To maximize class discrimination and biomarkers, the data were further analyzed using the OPLS-DA method. S-plots were calculated to visualize the relationship between covariance and correlation within the OPLS-DA results. Variables that had significant contributions to discrimination between groups were considered as potential biomarkers and subjected to further identification of the molecular formula.

2.6 Biomarkers identification and construction of metabolic pathway

By comparing their mass spectra and chromatographic retention times with the available reference standards, the potential biomarkers were comprehensively identified. The complete spectral information was obtained in the positive ion mode. The Mass Fragment application manager (Waters MassLynx v4.1, Waters corp., Milford, MA) was used to facilitate the MS/MS fragment ion analysis process by way of chemically intelligent peak-matching algorithms. The information is submitted to the database search, either internally or using the online database. (www. chemspider.com), and Mass Bank (http:// www.massbank.jp/), PubChem (http://ncbi.nim.nih.gov/) data source.

The construction, interaction, and pathway analysis of potential biomarkers was performed with MetPA (http://metpa. metabolomics.ca./MetPA/faces/Home.jsp) based on database source including the KEGG (http://www.genome.jp/kegg/), Human

Metabolome Database (http://www.hmdb.ca/) for identification of the affected metabolic pathways and visualization.

2.7 Isolation of peripheral blood mononuclear cells (PBMC)

Peripheral blood was taken from healthy volunteers. Mononuclear cells were isolated in a Ficoll–Hypaque (Pharmacia, Piscataway, NJ) (Pervin et al., 2015,) density gradient using standard procedures. The buffy coat containing PBMCs was removed carefully following centrifugation and washed twice in RPMI 1640 medium containing 10% FCS (Sigma). Cells were counted and assessed for viability.

2.8 Real-time quantitative PCR

Total RNA was isolated from treated PBMCs using Trizol reagent (Sigma, St Louis, MO, USA) following the protocol provided by the manufacturer. Real-time quantitative PCR was performed by using SYBR Green Master mix and Rox reference dye, according to the manufacturer's instructions. The cDNAs were obtained from the reverse transcription of the RNA from rat brain tissues and astrocyte cells. The primers were listed below. SYBR green signal was detected by Mx3000ptm multiplex quantitative PCR machine. Transcript levels were quantified by using the ΔΔCt value method (Schmittgen et al., 2002). Calculation (Bahman et al., 2012) was done by using the Ct value of GAPDH to normalize the Ct value of target gene in each sample to obtain the ΔΔCt value, which then used to compare among different samples. PCR products were analyzed by gel electrophoresis on a 1.5% agarose gel, and the specificity of amplification was confirmed by the melting curves.

2.9 Western blot analyses

PBMC were treated with the optimized doses of paeoniflorin for the required time points. The cells were lysed with extraction buffer (20 mM HEPES, 150 mM NaCl, 1% Triton X-100, 1 mM EDTA, 1 mM PMSF, 10 Ag/ml leupeptin, and 10 Ag/ml aprotinin). After 30 min at 4-8 °C, debris was eliminated by centrifugation at 14,000 rpm for 20 min, and the supernatant was collected. Cell lysates were separated by 10% SDS-PAGE, transferred to polyvinylidene difluoride membranes, and blocked with 0.05% Tween 20 and 5% BSA overnight. The immunoblots were incubated with anti-phospho-specific extracellular signal-regulated kinase (ERK) Ab, anti-ERK Ab, anti-phospho-specific p38 Ab, anti-p38 rabbit Ab, anti-phospho-specific JNK rabbit Ab, or anti- JNK rabbit polyclonal Ab in PBS with 1% BSA for 1 h. Subsequently, the immunoblots were incubated with secondary antibody conjugated with HRP in 1% BSA in PBS, 0.1% Tween 20. After 1h incubation at room temperature the bands are detected using chromogenic substrate.

2.10 Compliance with ethical requirements

All experimental protocols were approved by Medicine Ethics Review Committee for animal experiments of Nanjing University of Chinese Medicine. The methods were performed in accordance with the approved animal protocols and guidelines established.

3. Results

3.1 Biochemical indicators analysis

Biochemistry data was presented in Table 1. The levels of indicators were changed significantly after the treatment of SFZYD ($p < 0.05$ or $p < 0.01$). For hormone

indicators, SFZYD reduced significantly the levels of Estradiol ($P < 0.01$), and SFZYD obviously increased the levels of Progesterone ($p < 0.05$). The elevated inflammatory factors levels of $PGF_{2\alpha}$ and Endothelin were inhibited significantly, and that of β-endorphin was increased significantly after the treatment of SFZYD ($p < 0.05$). The elevated neuro-transmitter Oxytocin was reduced significantly ($p < 0.05$). These data implied that SFZYD regulated multiple biochemical indicators related to neuro-endocrine-immune (N-E-I) system and exhibited an integral efficacy.

3.2 LC-MS Analysis of metabolic profiling

Typical based peak intensity (BPI) chromatograms of plasma and urine samples, collected from diseased rats and normal rats in positive modes were different. A total of 296 ions in plasma samples and 325 ions in urine samples at positive modes were detected from diseased rats and normal rats. The supervised OPLS-DA divided samples into two blocks: Better discrimination between the two groups was obtained by this method. Based on the differences in their metabolic profiles, the OPLS-DA score plot analysis distinguished the plasma and/or urine samples of diseased rats and normal rats. The results of different pattern recognition indicated that endogenous metabolites change as a result of PD. From and loading plots, 39 ions in the plasma and urine samples of 58 ions in the positive mode were treated as discrimination ($p < 0.05$), and identified as being responsible for the separation between diseased rats and normal rats (Figure. 2). Finally, twenty-five potential biomarkers (ten in plasma and fifteen in urine) were tentatively identified.

3.3 Identification of potential biomarkers and Metabolic pathway function analysis

In the plasma, ten endogenous metabolites, were identified by comparing with authentic standards or based on their molecular ion information as well as the fragments of corresponding product ion (Table 2). The precise molecular mass was determined within measurement errors (<5 ppm) by Q-TOF. Compared with normal rats, there are up regulated metabolites in diseased rats, including LysoPC(22:6(4Z,7Z,10Z,13Z,16Z,19Z)), L-Acetylcarnitine, L-Threonine, PC(18:1(9Z)/16:1(9Z)), Deoxycholic acid 3-glucuronide ($p < 0.05$). While the significantly down regulated ones were LysoPC(18:0), LysoPE(20:0/0:0), LysoPE(22:0/0:0), LysoPC(P-18:1(9Z)), LysoPC(20:1(11Z)) ($p < 0.05$) (Table 3).

Fifteen endogenous metabolites were initially identified as described above. The metabolites of Cortisol, Glycyl-glycine, N-Acetylneuraminate 9-phosphate, 3α,21-Dihydroxy-5β-pregnane-11,20-dione, Androstenedione, trans-3- Octenedioic acid, Corticosterone, Creatine, Indole-3- carboxylic acid were observed to be up regulated significantly ($p < 0.05$), whereas the metabolites of 2-Oxoarginine, *trans*-3-Octenedioic acid, 2-Octenedioic acid, 3-Hydroxymethylglutaric acid, 3-Indolebutyric acid, 5-Hydroxy-L-tryptophan were down regulated obviously ($p < 0.05$). These differences in plasma and urine may be potential biomarkers for the differential diagnosis of PD and its normal state.

Here, an analysis of the metabolic pathways of MetPA revealed that the identification of biomarkers in plasma and urine is meaningful for primary

dysmenorrhea, which was responsible for pentose and glucuronate interconversions, and glycerophospholipid metabolism, steroid hormone biosynthesis, and tyrosine metabolism were disturbed when PD occurred. The pathway impact value calculated from pathway topology analysis above 0.1 was filtered out as potential target pathway.

3.4 Intervention effects of SFZYD

In order to clarify the effect of SFZYD intervention, PCA analysis was carried out to obtain the changes between diseased rats and treated rats. The variations of urine metabolic profiling of SFZYD-treated rats was restored back to the normal levels on the eighth day (Figure. 3). Furthermore, eight endogenous metabolites in plasma and thirteen endogenous metabolites in urine were significantly affected by SFZYD ($p < 0.05$ or $p < 0.01$). And all these metabolites were restored back to a normal level and there is no significant difference between the SFZYD- treated group and normal controls ($p > 0.05$) except for M8, M9 and M19, M22.

3.5. Correlation analysis between biomarkers and biochemistry indicators

Pearson correlation matrix analysis was used to discover the correlations between potential biomarkers and biochemical indicators (Figure. 4). The results indicated that the level of *β*-endorphin was strong positive associated with metabolites of M5 (Deoxycholic acid 3-glucuronide, r= 0.642) and M7 (LysoPE(20:0/0:0), r = 0.674). PGF_2 was significantly positive associated with M23 (3-Hydroxymethylglutaric acid, r = 0.939) and negative associated with M12 (Glycyl-glycine, r = -0.685) and M21 (*trans*-3-Octenedioic acid, r = -0.594). Oxytocin and progesterone were significantly

negative associated with M1 (LysoPC(22:6(4Z,7Z,10Z,13Z,16Z,19Z)), r = -0.942 and r= -0.626, respectively) and M9 (LysoPC(P-18:1(9Z)), r = -0.633 and r = -0.731, respectively). The level of Endothelin was significantly negative associated with metabolites of M7 (LysoPE(20:0/0:0), r = -0.635), M16 (*trans*-3-Octenedioic acid, r = -0.571), M22 (2-Octenedioic acid, r = -0.618) and M25 (5-Hydroxy-L-tryptophan, r = -0.708). An obvious negative correlation was discovered between inflammatory mediators of Estradiol and M23 (3-Hydroxymethylglutaric acid, r = -0.733) and positive associated with M12 (Glycyl-glycine, r = 0.596), respectively. These correlationships could be valuable for understanding the CPD related with Tyrosine metabolism and steroid hormone disorder.

3.6. Effect of paeoniflorin on cytokine transcription in phytohaemagglutinin (PHA) stimulated-PBMC

To determine the optimal concentration of Paeoniflorin, different concentrations of Paeoniflorin were incubated with PBMC to observe its inhibitory effect. This inhibition was not due to its direct toxicity on cells, which was confirmed by MTT assay at 24 h (Table-4). Based on the above data, 3 μg/ml was selected as optimal doses for Paeoniflorin and was used for further analysis. The results of PHA activated PBMC experiments showed that PHA stimulated-PBMC can enhance the transcription of these cytokines, and paeoniflorin can inhibit the expression of these cytokines (Fig. 5).

3.7 Response of MAPK on treatment with paeoniflorin

Mitogen activated protein kinases (MAPK) are central to many immune responses, including the regulation of cytokine responses, chemokine responses and cell proliferation. To understand the mechanism by which regulates lymphocyte proliferation and inflammatory mediators, the effects of paeoniflorin on MAPK activities were evaluated. PBMC were stimulated with PHA and ionomycin for 3 and 6 h to activate these MAPK. The effect of paeoniflorin on MAPK was assessed by Western blotting (Fig. 6). Using antibodies that specifically recognize phosphorylated forms of ERK, JNK and the p38, the kinetics of MAPK activation in the presence of paeoniflorin was evaluated. At these time points co-incubation of PBMCs with paeoniflorin resulted in considerable reduction in phosphorylated forms of all the three MAPK (ERK1/2, p38 and JNK).

Studies have described PHA can active MAPK signaling pathway cascades in PBMC and we hypothesized that paeoniflorin could disrupt this pathway exerting its effects. Our subsequent western blot assays showed that the phosphorylation of ERK, JNK and p38 was significantly enhanced in the activation of PHA, but paeoniflorin led to a significant reduction in the phosphorylated ERK, JNK and p38 (Fig. 6).

3.8 Down regulation of *c-jun* and *c-fos*

PBMCs treated with Paeoniflorin showed marked inhibition of both c-jun and c-fos expression (Fig. 5). The marked reduction in c-jun levels could affect AP-1 levels and thereby the downstream signals resulting in inhibition of inflammatory cytokines.

4. Discussion

In this study, metabolomics were applied to investigate changes of the comprehensive metabolic characters and biomarkers in plasma and urine of CSBS primary dysmenorrhea diseased rats. Metabolic profiling technique has been considered as an effective means for the identification of the relative amount of metabolites, which is altered in response to disease or therapeutic intervention. It was implied that the pathways of pentose and glucuronate interconversions, glycerophospholipid metabolism and steroid hormone biosynthesis in plasma and urine were disturbed, respectively. After the treatment with SFZYD, these disturbed metabolic profiling was restored back to the control-like levels. In addition, twenty-one SFZYD regulated specific metabolites were identified. These promising biomarkers candidates verified that the pathogenesis of PD is closely related to multiple etiologies and pathogenesis.

PD has been suggested to be a sex-hormone related disorder: there is a buildup of fatty acids in the phospholipids of the cell membranes (Cornel et al., 2012). After the onset of progesterone withdrawal before menstruation, these omega-6 fatty acids, particularly arachidonic acid, are released, and a cascade of prostaglandins (PG) and leukotrienes (LT) is initiated in uterus. LT is proinflammatory mediators of inflammation. Therefore, compared with normal rats, there are up regulated metabolites in diseased rats, including Deoxycholic acid 3-glucuronide. The PGF2α, cyclooxygenase (COX) metabolite of arachidonic acid, caused potent vasoconstriction

and myometrial contractions such as trans-3- Octenedioic acid, which was leading to pain(Harel., 2002).

Cytokines produced by T cells and macrophages such as IL-1β, IL-2, IL-10, IL-12, TNFα and INFγ are known to play a central role in initiating and perpetuating a variety of inflammatory and autoimmune disorders. When the profile of cytokine secretion by activated T cells and macrophages were analyzed, it was revealed that paeoniflorin significantly suppressed these inflammatory cytokines (Fig. 4). To understand the mechanism by which paeoniflorin regulates inflammatory mediators, its effect on mitogen activated protein kinases (MAPK) was assessed. MAP kinases are critical in immune and inflammatory process regulating the expression of a wide variety of cytokines including IL-1β, IL-2, IL-10, IL-12, TNF-α and INF-γ (Swantek et al., 1997; Rao et al., 2002). Its ubiquitous distribution, rapid induction and its apparent involvement in several diseases have made this pathway a potential target for the treatment of inflammatory disorders (Hommes et al., 2003). MAP kinases, signal transduction pathways in mammalian cells, include the extracellular signal related kinase (ERK), *c-Jun* N-terminal kinase (JNK/SAPK) and p38 MAP kinase. The presence of all the three kinases has been shown to play a critical role in the events leading to inflammatory cytokines production (Su et al., 1994). ERK, JNK and p38 MAP kinases are regulated by paeoniflorin in PHA stimulated PBMCs (Fig. 5).

The inflammatory response, mediated by these PGs and LTs, produces both cramps and systemic symptoms such as nausea, vomiting, bloating and headaches. The PGF2α, cyclooxygenase (COX) metabolite of arachidonic acid, caused potent

vasoconstriction and myometrial contractions, which was leading to ischemia and pain. In our study, three unique metabolic pathways of pentose and glucuronate interconversions, glycerolphospholipid metabolism, and steroid hormone biosynthesis were identified from diseased rats. Furthermore, potential biomarkers of Androstenedione were identified. It has been found to have some functions in cell signaling and specific receptors (coupled to G proteins). The correlation analysis results showed that the levels of endothelin was closely related to the metabolites of LysoPE(20:0/0:0) and creatinine and which agreed with the reports of literatures (Schumacher et al., 2007). The correlations of biomarkers and biochemical indicators could be significant for the elucidation of PD pathogenesis. More importantly, these promising biomarkers could provide guidance for clinical diagnosis and therapy of PD. This result may indicate that the profile of the metabolomics was closely correlated to traditional biological and clinical end points, and was thus becoming a useful tool for diagnosis and evaluation of therapy.

5. Conclusion:

These findings indicated that SFZYD improved the metabolic profiling and biochemical indicators on CSBS primary dysmenorrhea rats. And the mechanisms were closely related with the regulation of the MAPK pathway by reduction in phosphorylated forms of the three MAPK (ERK1/2, p38 and JNK) and down regulation of *c-jun* and *c-fos* by paeoniflorin. The data could be provided the guidance for further research and new drug discovery.

Acknowledgments

The authors wish to acknowledge Dr. Yue Zhu for technical support with qRT-PCR and Western Blot experiment.

Author contributions

XCH and SLS conceived and designed the project, with input from JAD, XXS, KYZ, JMG. PL, DWQ, XCH, XXS, LY and EXS performed experiments. SLS and XXS planned and supervised mouse experiments. XCH, SLS and JAD wrote the manuscript, with contributions from all authors.

Reference

Balkwill, F., Mantovani, A., 2001. Inflammation and cancer: back to Virchow? Lancet. 357, 539–545.

Baggio, V., Ott, F., Fische,r R.W., 2005, Production of antibodies to canine IL-1beta and canine TNF to assess the role of pro-inflammatory cytokines. Immunol. Immunopathol. 107, 27–39.

Bahman, N., Juan, B.L., Mohammad, F. J., 2012, Correlation Coefficients Between Different Methods of Expressing Bacterial Quantification Using Real Time PCR. J. Mol. Sci. 13, 2119-2132.

Cheng, Q.Q., Zhu, Y., 2011. Clinical study on primary dysmenorrheal of blood - stasis of cold-coagulation syndrome treated with modified Shaofu Zhuyu decoction. J. Chin. Med. 16, 1249−1250.

Chan, W.Y., Dawood, M.Y., 1980. Prostaglandin levels in menstrual fluid of non dysmenorrheic and of dysmenorrheic subjects with and without oral contraceptive or Ibuprofen therapy. Adv. Prostaglandin. Thromboxane. Res. 8, 1443−1447.

Cornel, K.M., Kruitwagen, R.F., Delvoux, B., 2012, Overexpression of 17β-hydroxysteroid dehydrogenase dehydrogenase type 1 increases the exposure of endometrial cancer to 17β-estradiol, J. Clin. Endocrinol. Metab. 97, 591−601.

Doubova, S.V., Morales, H.R., Hernandez, S.F., 2007. Primary dysmenorrhea in adolescent girls and treatment with oral contraceptives. J. Ethnopharmacol. 110, 305–310.

Davis, A.R., Westhoff, C., O'Connell, K. 2005. Oral contraceptives for dysmenorrhea in adolescent girls: a randomized trial. J. Pediatr. Adolesc. Gynecol. 106, 97−104.

Fan. M., 2011. Clinical observation of Shaofu Zhuyu decoction for treating primary dysmenorrhea of cold coagulation and blood stasis. Beijing J Trad Chin Med. 30, 455−456.

French, L., 2005. Nonsteroidal anti-inflammatory drugs and hormonal contraceptives for pain relief from dysmenorrhea: a review. Am. Fam. Physician. 71, 285−291.

Hsu, C.S., Yang, J.K., Yang, L.L., 2006. Effect of "Dang-Qui-Shao-Yao-San" a Chinese medicinal prescription for dysmenorrhea on uterus contractility in vitro, Phytomedicine. 13, 94-99.

Hommes, D.W., Peppelenbosch, M.P., Deventer, S.J., 2003. Mitogen activated protein (MAP) kinase signal transduction pathways and novel anti-inflammatory targets, Gut. 81, 144– 51.

Hougee, S., Sanders, A., Faber, J., 2005. Decreased pro-inflammatory cytokine production by PS-stimulated PBMC upon in vitro incubation with the flavonoids apigenin, luteolin or chrysin, due to selective elimination of monocytes/macrophages. Biochem. Pharmacol. 69, 241–248.

Harel, Z. A., 2002. Contemporary approach to dysmenorrhea in adolescents. Paediatr. Drugs. 12, 797−805.

Kracht, M., Saklatvala, J., 2002. Transcriptional and post-transcriptional control of

gene expression in inflammation. Cytokine. 20, 91–106.

Liu, P., Duan, J.A., Wang, P.J., Qian, D.W., 2013. Biomarkers of primary dysmenorrhea and herbal formula intervention: an exploratory metabonomics study of blood plasma and urine. Mol. BoiSyst. 9, 77-87.

Moss, S.F., Blaser, M.J., 2005, Mechanisms of disease: inflammation and the origins of cancer, Clin. Pract. Oncol. 2, 90–97.

Nicholson, J.K., Everett, J.R., Lindon, J.C., 2012. Longitudinal pharmacometabonomics for predicting patient responses to therapy: drug metabolism, toxicity and efficacy. Drug Metab Toxicol. 8, 135–139.

Ostad, S.N., Soodi, M., Shariffzadeh, M., 2001. The effect of fennel essential oil on uterine contraction as a model for dysmenorrhea, pharmacology and toxicology study. J. Ethnopharmacol. 76, 299-305.

Proctor, M.L., Roberts, H., Farquhar, C.M., 2001. Combined oral contraceptive pill (OCP) as treatment for primary dysmenorrhoea. Cochrane Database Systematic. Reviews. 4, CD002120.

Pevin, R., Erkan, R., Adile, Ç., 2015. Effect of Antibiotics on Polymorphonuclear Leukocyte Functions and Myeloperoxidase Activity, Glutathione and Malondialdehyde Levels in Allergic Asthma. 64, 69-72.

Rao, K.M., Meighan, T., Bowman, L., 2002. Role of mitogen-activated protein kinase activation in the production of inflammatory mediators: differences between primary rat alveolar macrophages and macrophage cell lines. J Toxicol Environ Health. 65, 757– 68.

Su, S.L., Hua, Y.Q., Duan, J.A., 2010, Inhibitory effects of active fraction and its main components of Shaofu Zhuyu decoction on uterus contraction. J. Chin. Med. 38, 777−787.

Su, S.L., Guo, J.M., Duan, J.A., 2010. Ultra-performance liquid chromatographytandem mass spectrometry analysis of the bioactive components and their metabolites of Shaofu Zhuyu decoction active extract in rat plasma. J. Chromatog.r B. 878, 355−362.

Su, S.L., Duan, J.A., Wang, P., 2013. Metabolomic Study of Biochemical Changes in the Plasma and Urine of Primary Dysmenorrhea Patients Using UPLC−MS Coupled with a Pattern Recognition Approach. J. Proteome. Res. 12, 852−865.

Stener-Victorin, E., Holm, G., Labrie, F., 2010. Are There Any Sensitive and Specific Sex Steroid Markers for Polycystic Ovary Syndrome?. J. Clin. Endocrinol. Metab. 95, 810–819.

Schmittgen, T.D., Zakrajsek, B.A., Mills, A.G., 2002, Quantitative reverse transcription-polymerase chain reaction to study mRNA decay: comparison of endpoint and real-time methods. Anal. Biochem. 85, 194–204.

Swantek, J.L., Cobb, M.H., Geppert, T.D., 1997. Jun N-terminal kinase/stress-activated protein kinase (JNK/SAPK) is required for lipopolysaccharide stimulation of tumor necrosis factor alpha (TNF-alpha) translation: glucocorticoids inhibit TNF-alpha translation by blocking JNK/SAPK. Mol. Cell. Biol. 17, 6274– 82.

Su, B., Jacinto, E., Hibi, M., 1994. JNK is involved in signal integration during

costimulation of T lymphocytes. Cell. 77, 727–736.

Schumacher, M., Guennoun, R., Ghoumari, A., 2007. Novel perspectives for progesterone in hormone replacement therapy, with special reference to the nervous system. Endocr Rev. 28, 387−439.

Wolf, L.L., Schumann, L., Acad, J.A. 1999. Prostaglandin levels in menstrual fluid of non dysmenorrheic and of dysmenorrheic subjects with and without oral contraceptive or Ibuprofen therapy. Adv. Nurse. Pract. 11, 125-132.

White, F.A., Bhangoo, S.K., Miller, R.J., 2005. Chemokines: integrators of pain and inflammation. Nat Rev Drug Discov. 4, 834–844.

Yan. L., Anderson, G.M., DeWitte, M., 2006, Therapeutic potential of cytokine and chemokine antagonists in cancer therapy. Eur. J. Cancer. 42, 793-802.

Zahradnik, H.P., Hanjalic-Beck, A., Groth, K., 2010. Nonsteroidal anti-inflammatory drugs and hormonal contraceptives for pain relief from dysmenorrhea: a review. Contraception. 81, 185−196.

Figure Legends

Figure 1 PCA model results between diseased rats and normal rats in positive mode. (A, 2-D plot of urine; B, 2-D plot of plasma; C, 3-D plot of urine; D, 3-D plot of plasma)

Figure 2 S-plot of OPLS-DA model for diseased vs normal rats. (A, urine; B, plasma).

Figure 3 PCA analytical results from diseased rats treated with SFZYD at positive mode for urine.

Figure 4 Correlation analysis between biomarkers and biochemistry data in plasma before dministration of SFZYD , Rows, metabolites; Columns, biochemical indicators; Color key indicates correlation value: blue, lowest; red, highest. The correlation heat-map was built and optimized by MATLAB software (MathWorks, US).

Figure 5 Analysis of Paeoniflorin on PHA induced proinflammatory cytokine and *c-fos* and *c-jun* expression in PBMC. PBMCs were induced with PHA (10 ng/ ml) for 6 hours and inhibitory effect of Paeoniflorin on cytokines and *c-fos* and *c-jun* expression was studied by RT-PCR analysis.

Figure 6 Analysis of Paeoniflorin on MAPK. A) non-phospho ERK, B) Phospho-ERK, C) non-phospho JNK, D) Phospho-JNK, E) non-phospho p38, F) Phospho-p38. By Western blotting, the inhibitory effects of crude ethyl acetate extract and pure compound on active forms of MAP kinases were analysed in PHA stimulated PBMC, using antibodies recognizing the phosphorylated and non-phophorylated forms of ERK1/2, JNK and p38 MAPK.

Table captions

Table 1 Level of Biochemical Indicators in Serum of model rats before and after the Treatment by SFZYD (mean ± SD, n = 8).

indicator	Normal group	Diseased group	SFZYD group	*P* value
estradiol	8.04±0.86	15.2±1.19	9.30±0.22	0.0024
oxytocin	1.56±0.17	2.97±0.25	1.94±0.09	0.0003
progesterone	2.01±0.06	1.05±0.08	2.20±0.07	0.0020
endothelin	9.86±0.40	25.31±0.48	15.93±0.38	0.0000
β-endorphin	44.44±2.23	25.02±0.55	39.16±4.68	0.0000
$PGF_{2\alpha}$	2.55±0.03	7.10±0.20	3.46±0.21	0.0000

Table 2 Identified Differential Metabolites Accountable for the Discrimination between dieased rats and nomal rats in Plasma.

no	t_R	metabolites	obsd $[M+H]^+$	calcd [M+H]+	Content variance[d]	pathway
M1	8.66	LysoPC(22:6(4Z,7Z,10Z,13Z,16Z,19Z))	568.3398	567.3325	↑	
M2	1.82	L-Acetylcarnitine	204.1230	203.1158	↑	
M3	7.57	L-Threonine	120.0655	119.0582	↑	Glycerophospholipid metabolism
M4	3.17	PC(18:1(9Z)/16:1(9Z))	610.5694	609.5622	↑	Pentose and glucuronate interconversions
M5	8.66	Deoxycholic acid 3-glucuronide	569.3320	568.3247	↑	
M6	6.62	LysoPC(18:0)	524.3711	523.3638	↓	Glycerophospholipid metabolism
M7	8.35	LysoPE(20:0/0:0)	510.3554	509.3481	↓	
M8	6.43	LysoPE(22:0/0:0)	538.3867	537.3794	↓	
M9	7.51	LysoPC(P-18:1(9Z))	506.3605	505.3532	↓	
M10	8.96	LysoPC(20:1(11Z))	550.3867	549.3794	↓	

Table 3 Identified Differential Metabolites Accountable for the Discrimination between diseased rats and nomal rats in Urine.

no	t_R	metabolites	obsd $[M+H]^+$	calcd [M+H]+	Content variance[d]	pathway
M11	5.89	Cortisol	363.2166	362.2093	↑	
M12	8.86	Glycyl-glycine	133.0608	132.0535	↑	
M13	8.48	N-Acetylneuraminate 9-phosphate	390.0796	389.0723	↑	
M14	8.29	3*α*,21-Dihydroxy-5*β*-pregnane-11,20-dione	349.2373	348.2301	↑	Steroid hormone biosynthesis
M15	4.94	Androstenedione	287.2006	286.1933	↑	Steroid hormone biosynthesis
M16	9.93	trans-3-Octenedioic acid	173.0808	172.0736	↑	
M17	11.15	Corticosterone	347.2217	346.2144	↑	Steroid hormone biosynthesis
M18	2.68	Creatine	132.0768	131.0695	↑	Steroid hormone biosynthesis
M19	3.57	Indole-3-carboxylic acid	162.0550	161.0477	↑	
M20	5.32	2-Oxoarginine	174.0873	173.0800	↓	
M21	9.93	trans-3-Octenedioic acid	173.0808	172.0736	↓	
M22	5.32	2-Octenedioic acid	173.0808	172.0736	↓	
M23	11.26	3-Hydroxymethylglutaric acid	163.0601	162.0528	↓	
M24	4.62	3-Indolebutyric acid	204.1019	203.0946	↓	
M25	8.29	5-Hydroxy-L-tryptophan	221.0921	220.0848	↓	

Table 4 The optical density(OD) of Control group and Paeoniflorin group by MTT.

Groups	Dosage(mg/ml)	OD(mean±SD)
Control group	---	0.663 ±0.039
Paeoniflorin	0.0015	0.693± 0.024
	0.0030	0.646 ±0.023
	0.0060	0.590 ±0.003
	0.0122	0.571 ±0.020
	0.0241	0.521 ±0.008

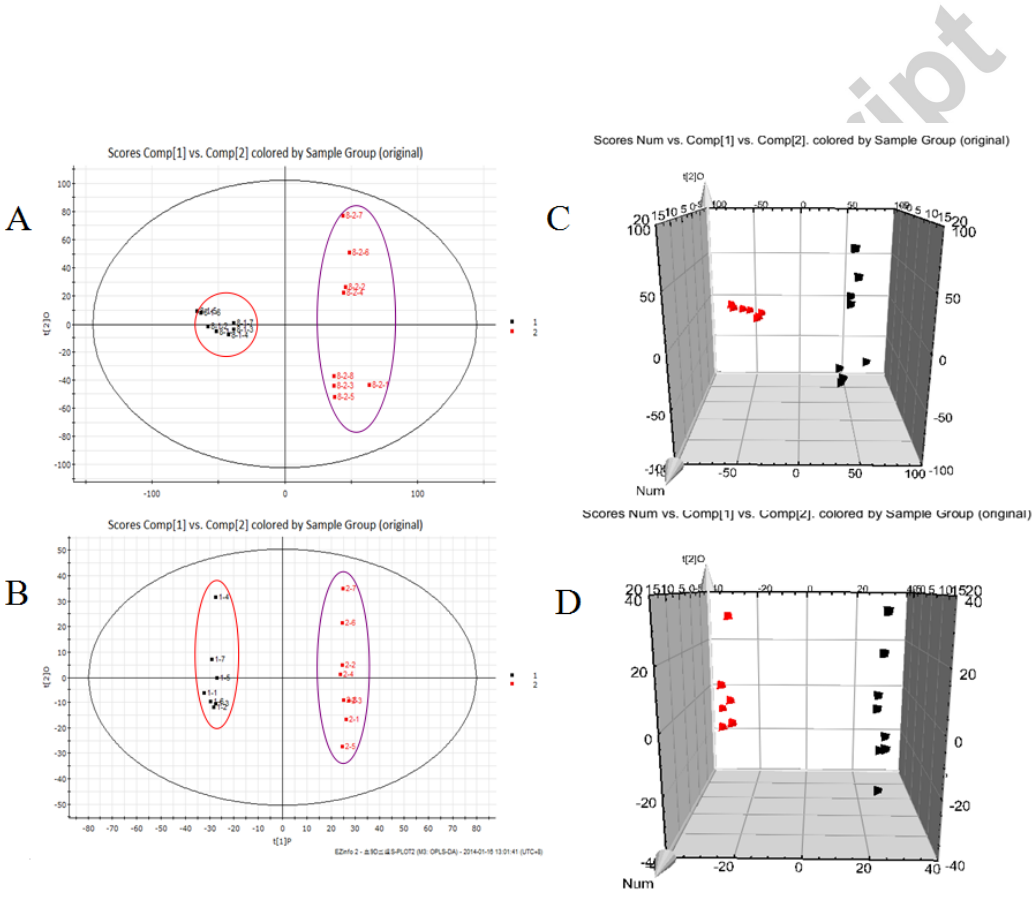

Figure. 1 Huang *et al 2015*

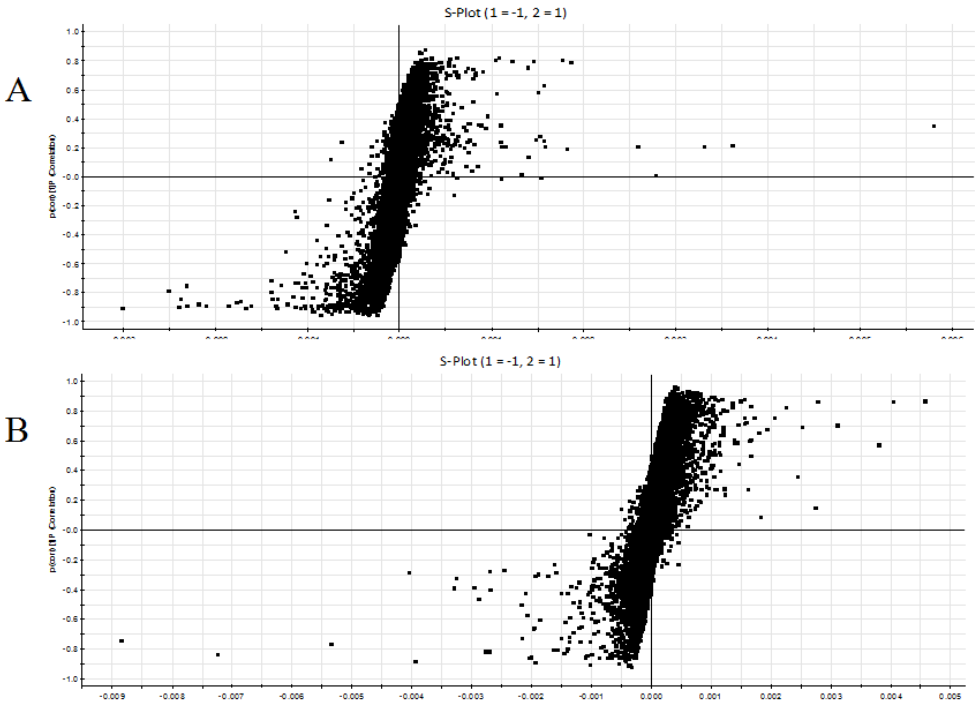

Figure. 2 Huang *et al 2015*

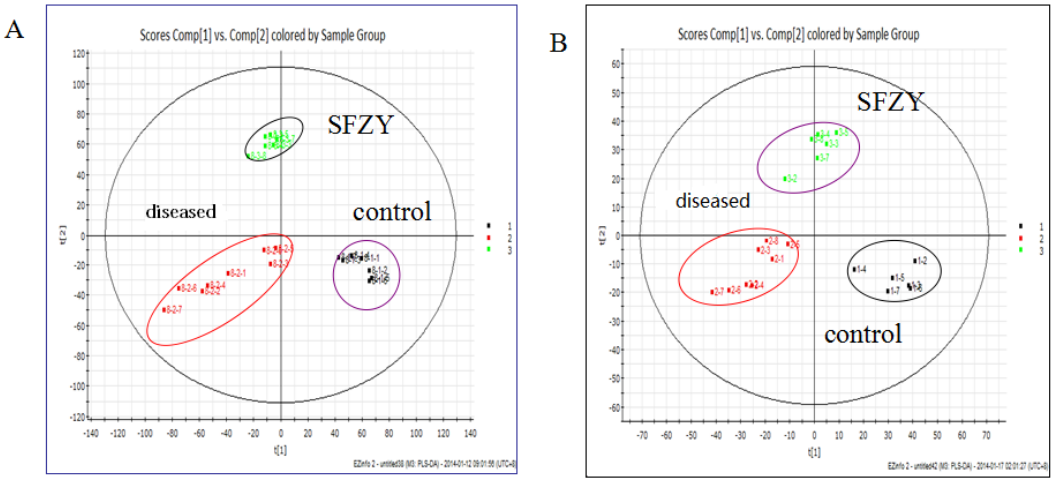

Figure. 3 Huang *et al 2015*

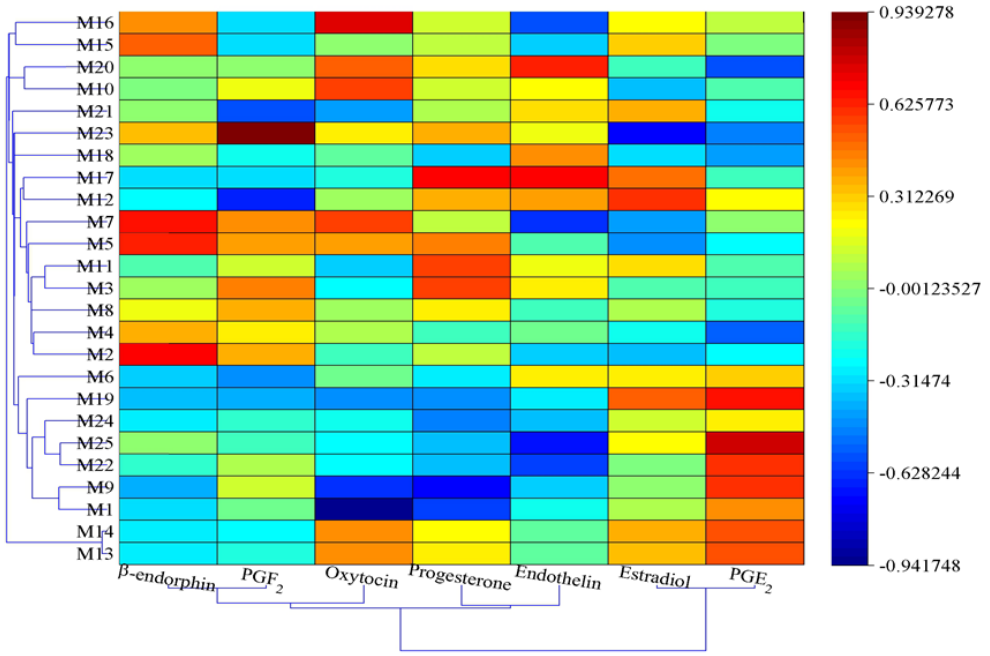

Figure. 4 Huang *et al 2015*

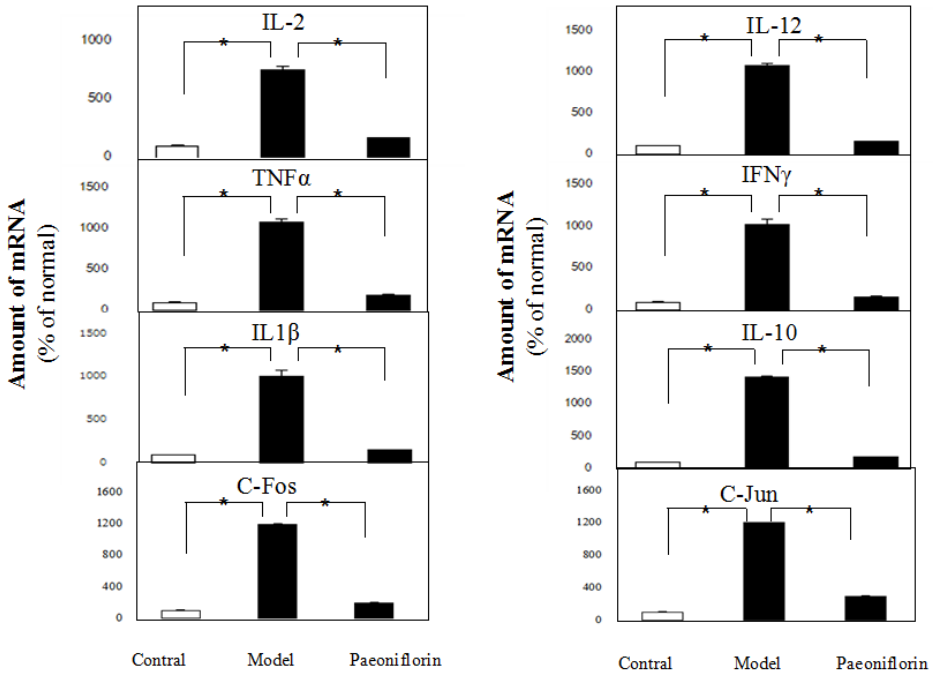

Figure. 5 Huang *et al 2015*

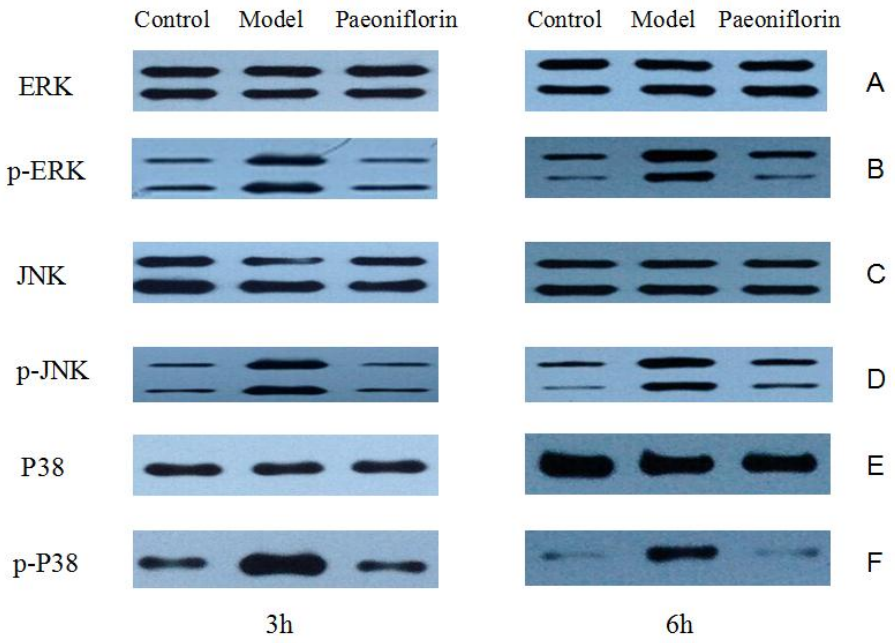

Figure.6 Huang *et al 2015*

Graphical abstract

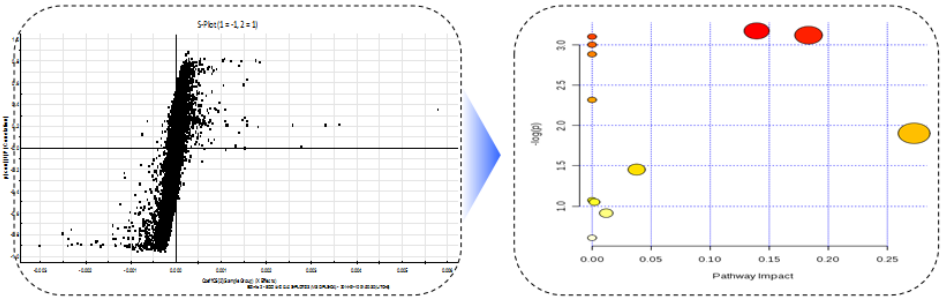

	Pathway Name	Total	Hits	p	-log(p)	FDR
A	Steroid hormone biosynthesis	0.7989	3	0.0418	3.1745	0.9048
B	Glycerophospholipid metabolism	0.3424	2	0.0441	3.1211	0.9048
C	Pentose and glucuronate interconversions	0.1598	1	0.1491	1.9032	1.0
	Starch and sucrose metabolism	0.26248	1	0.2336	1.454	1.0
	Arachidonic acid metabolism	0.41084	1	0.3419	1.0731	1.0